IEEE Journal of Microwaves

Received 23 October 2021; revised 28 November 2021; accepted 28 November 2021. Date of publication 15 December 2021; date of current version 7 January 2022.

Digital Object Identifier 10.1109/JMW.2021.3131844

Vehicle Platform Effects on Performance of Flexible, Lightweight, and Dual-Band Antenna for Vehicular Communications

ADAMANTIA CHLETSOU [1] (Student Member, IEEE), JOHN F. LOCKE [2], AND JOHN PAPAPOLYMEROU [1] (Fellow, IEEE)

(Regular Paper)

[1]Electrical and Computer Engineering Department, Michigan State University, East Lansing, MI 48824 USA
[2]Ford Motor Company, Dearborn, MI 48126 USA

CORRESPONDING AUTHOR: Adamantia Chletsou (e-mail: chletsou@egr.msu.edu).

ABSTRACT This paper highlights the impact of the ground, of the vehicle surroundings and of the car body on signal transmission and reception of a dual-band microwave antenna tested on two automotive plastic parts on a convertible vehicle for cellular and Cellular - Vehicle To Everything (C-V2X) communications. The implemented antenna operates at 975 MHz and 5.5 GHz and facilitates the future vehicular communications in vehicles without steady rooftops. Four experiments are performed with the antenna placed (a) in the Satimo near field system; (b) on a stanchion at an outdoor range facility without the presence of a car; (c) at the outdoor facility in the side mirror of the convertible vehicle; and (d) on the trunk lid of the same vehicle. Antenna co- and cross- polarization radiation patterns are measured and results indicate that the ground and the vehicle's body affect the radiation performance of the antenna. The presence of ground causes an increase in the antenna's cross-polarization level. The reflections caused by the car's body perturb the omni-directional radiation pattern of the antenna and may degrade the vehicular microwave signal transmission due to the presence of nulls.

INDEX TERMS Antenna polarization, automotive antenna, autonomous vehicles, cellular frequencies, C-V2X frequencies, dual-band antenna, flexible antenna, microwave applications, side mirror, trunk lid.

I. INTRODUCTION

With the advent of fully autonomous vehicles, the number of antennas facilitating the vehicular wireless communications on a vehicle has increased dramatically. The large amount of antennas needed in combination with the limited space where an antenna can be placed on a vehicle due to its Perfect Electric Conductor (PEC)-like body has led researchers to focus on solutions like multi-band antennas where a single antenna can cover more than one bands, as well as investigating placements of an antenna throughout the whole car body and not restrict the antenna placement only at the vehicle's rooftop. But there is not significant research on the effect of the ground and the vehicle body on the signal of the antenna. This paper investigates the influence of the ground, the vehicle surroundings and the car body on the radiation performance of a dual-band antenna for C-V2X applications.

There is a lot of ongoing research on automotive antennas for Vehicle to Everything communications but most of the antennas are placed on the rooftop of the vehicle like in [1], [2], [3]. Antenna positions on a vehicle, similar to the mounting that is presented in this paper is used in [4]. The authors tested two dislocated antennas for satellite communications as a diversity antenna inside a vehicle's side mirror. The authors of [5] present a measurement-based analysis of the impact of antenna placement on vehicle-to-vehicle communications. In order to develop the desired analysis, the antenna was tested inside a vehicle's left side mirror, bumper, rooftop and windshield. In [6] a half wavelength dipole antenna is mounted on a right side mirror and the frequency of

TABLE 1. Comparison of This Work to the Literature

Reference	Antenna Dimensions (mm^3)	Resonance frequencies (GHz)	Maximum Realized Gain (dBi)
[4]	32*32*11 (set of 3 antennas)	2.332	5
[6]	25.4 (λ/2 dipole)	5.9	5 (only simulated)
[7]	8.8*1.65*0.035	5.9	3
[14]	120*70*0.1	800 5.9	1.68 4.6
This work	91.5*30*0.1	0.975 5.4	0.3 1.6

the transmitted wave is set to 5.8 GHz. The radiation patterns as simulated in ANSYS software are presented. A monopole is placed inside a truck mirror and tested in the lab without the vehicle's body in [7]. The authors of [8] placed a vehicle in an anechoic chamber and positioned two sets of antennas at the left and right side mirrors of the vehicle in order to test the efficacy of the antenna sub-arrays for robust satellite navigation. In [9] a Sirius-XM antenna operating at 2326 MHz is placed under the trunk lid and its radiation patterns as calculated by Mathematical Absorber Reflection Suppression (MARS) algorithm is compared with the measured radiation pattern at a far field setup at ATC GmbH premises.

Testing facilities for automotive antenna measurements similar to the ones used in this paper to investigate the effect of the ground and the vehicle body on the antenna signal have been employed in [10] where a Car-to-X antenna is placed on the rooftop of a vehicle. The authors of [11] tested a Nefer MIMO system on the rooftop of a car in an antenna radome with a car turntable inside. The difference between the literature and the research done in the presented paper is that the radome used in the literature is closed and not affected by external environmental factors. The authors of [12] investigate how and when it is important to consider the ground and the turn table effect in the simulation models for the evaluation and development of car antenna systems, the influence of the body shell and the influence of the glass curvature by testing an antenna operating within 50-300 MHz on a rooftop of a commercial vehicle. An evaluation method of LTE-car antennas is presented in [13] by measuring the Antenna Under Test (AUT) on a rooftop of a commercial vehicle, in a closed radome.

In Table 1 are presented the dimensions of the antenna developed in this paper against the antennas from the literature, their resonance frequencies and the values of the realized gains. A similar antenna design is proposed in [14]. Compared to [14], the antenna suggested in this paper is optimized to operate at the cellular and C-V2X frequencies while mounted on a plastic piece under the Rogers 3850 substrate. Also, the antenna in [14] was designed, implemented and standalone measurements of it in an Near Field system were performed. In contrast to [14], the antenna presented here is measured on automotive plastics on a real vehicle at an outdoor facility in order to investigate the effect of the vehicle body and the ground on the signal transmission and reception of a non-grounded antenna. Compared to [4], [6] and [7] the antenna presented here is dual-band, resonating at 975 MHz and 5.5 GHz. C-V2X applications use the 5.9 GHz. The antenna suggested here, when measured alone resonates around 5.5 GHz but when placed on an automotive plastic the resonance shifts to 5.9 GHz. Also, compared to the [4] in Table 1 it is only one structure operating in two different frequencies and thus it is more compact. In addition, none of the antennas in Table 1 have been tested in a real environment with a ground and a whole vehicle body. The maximum value of the presented antenna realized gain at 5.9 GHz is almost the half of the [7]. The antennas presented in [7] and [6] have higher gain than the antenna suggested in this paper since they are supporting only the C-V2X band. The presented antenna is dual-band and because of the size of the meander line and the feed-line its radiation pattern at 5.5 and 5.9 GHz is deteriorated.

All things considered, compared to the above mentioned papers, this research investigates how the ground and the vehicle's body affect the cross-polarization of the antenna radiation pattern at two different microwave bands (cellular and cellular vehicle to everything) at two positions on a commercial vehicle for the first time to the best of the authors' knowledge; 1) inside a vehicle's side mirror and 2) on the trunk lid of the same vehicle at the outdoor antenna range facilities managed by the Applied EMAG and Wireless Lab of Oakland University rather than performing standalone antenna measurements in an anechoic chamber.

Standalone antenna measurements, without the vehicle, on a stanchion are performed initially, in order to address the effect of the ground on the signal transmission and reception. On a second step the antenna is placed inside the right side-mirror of the convertible vehicle and at the last step the same antenna is placed on the trunk lid of the vehicle. The radiation patterns of the antenna with the vehicle are compared with the radiation patterns of the antenna without the car's body. Also, the patterns and the influence of the vehicle's body at these two different positions are investigated.

In Section 2, the design and the implementation method of the Antenna Under Test (AUT) are presented. In section 3, the measurements of: a) the antenna in a SATIMO chamber; b) the antenna on a stanchion, without the vehicle; c) the antenna with the vehicle and inside the right side-mirror; and d) the antenna with the vehicle and on the trunk lid at the outdoor facilities of the Oakland University are presented. In Section 4, the comparison among these measurements is demonstrated.

II. ANTENNA DESIGN AND SIMULATION RESULTS

The antenna is initially designed using Ansys EM (HFSS) software. The dual-band antenna consists of a bow-tie and two meander lines extending the bow-tie. It is fed by a slot-line, on which an SMA connector is soldered for measurements.

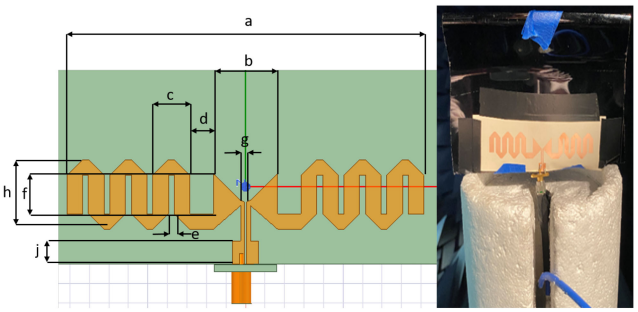

(a) (b)

FIGURE 1. (a) Simulated and (b) implemented antenna.

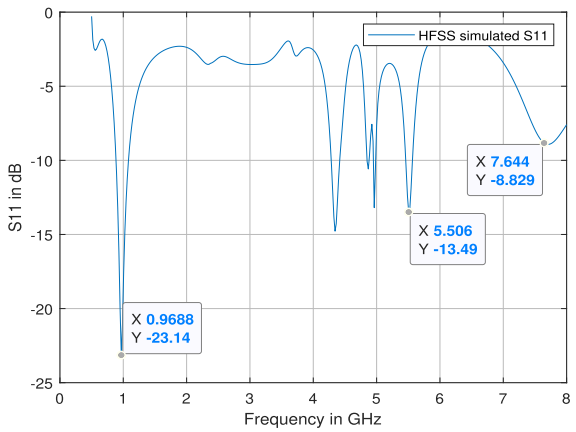

FIGURE 2. Simulated S_{11} in HFSS.

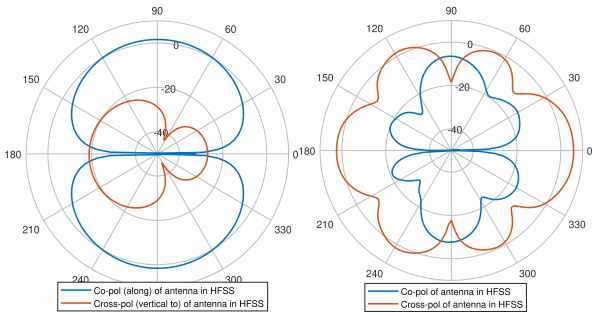

(a) (b)

FIGURE 3. Simulated co- and cross- polarization radiation patterns (a) at 968.8 MHz and (b) at 5.5 GHz.

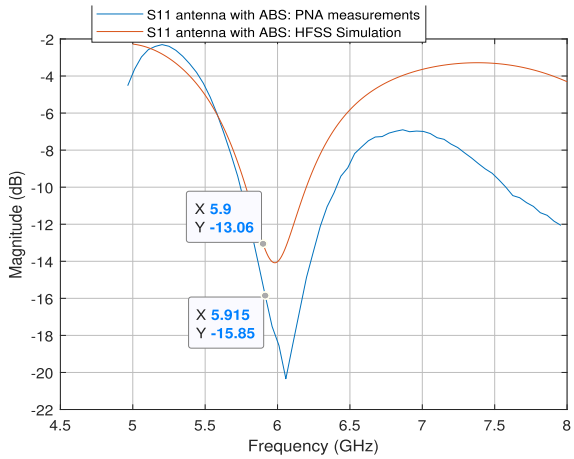

FIGURE 4. S_{11} as simulated in HFSS and measured in Satimo when there is ABS below the antenna.

The design is indicated in Fig. 1 and is inspired by the need for the antenna to resonate in two different frequencies. The bow-tie resonates close to C-V2X frequency bands and the extended meanders allow the antenna to operate at the lower cellular frequencies. The substrate of the antenna is the Rogers 3850 with a permittivity of $\epsilon_r = 2.9, tan\delta = 0.025$ and thickness t=1mil as stated in [15]. Most automotive plastics are created by Acrylonitrile Butadiene Styrene (ABS). The ABS has permittivity of $\epsilon_r = 2.5$ and $tan\delta = 0.004$. The dielectric characteristics of clear ABS parts are measured by the Agilent E4991 A RF Impedance Material Analyzer in the lab. In cellular frequencies the simulated antenna resonates at 968.8 MHz and for C-V2X applications, when the antenna is simulated alone, it resonates at 5.5 GHz as shown in Fig. 2. The simulated co- and cross-polarization radiation patterns of the antenna, without the ABS, at both frequencies, are indicated in Fig. 3. When an ABS part is added below the substrate, the measured resonance around 7.2 GHz shifts to 5.9 GHz, as indicated in Fig. 4. The resonance to a lower frequency when there is an ABS part below the antenna is expected since the permittivity of the material on which the antenna is mounted increases. As a result the effective wavelength λ_{eff} minimizes but the antenna length remains the same. So the antenna resonates to a lower frequency. The antenna was designed to operate with the ABS below the Rogers substrate. However, during the standalone antenna measurements this resonance shifts to 7.2 GHz and another resonance is created around 5.5 GHz. The required bandwidth for C-V2X applications is only 30 MHz extending from $5.895 - 5.925$ GHz. The simulated antenna with the ABS below the Rogers 3850 substrate is indicated in Fig. 5(a). It is obvious that the antenna is linearly polarized at the cellular frequencies but the cross-pol level is increased at 5.5 GHz and 5.9 GHz. At the lower frequency the antenna's dominant mode is TM since the antenna lies on xy plane in HFSS and the radiated field is mainly on the theta direction. However, at 5.5 GHz the antenna has a hybrid TE/TM mode. At 5.5 GHz and 5.9 GHz the length of the meander line as well as the size of the slot-line are not negligible when compared to the wavelength. As a result the antenna cross-pol level is increased by 15 dB when compared to the lower frequencies. The antenna has an omni-directional radiation pattern at 968.8 MHz as shown in Fig. 6(a) but loses the omni-directionality at 5.5 GHz due to the meander and the slot-line, as indicated in Fig. 6(b). At Fig. 7 the bow-tie antenna is simulated without the feed-line and the meander lines resulting in an omni-directional radiation pattern and

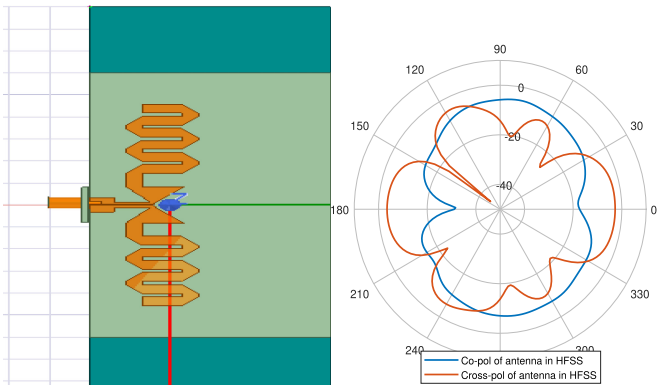

(a) (b)

FIGURE 5. **(a) Simulated antenna with ABS piece below the Rogers 3850 substrate (b) Simulated co- and cross- polarization radiation patterns at 5.9 GHz.**

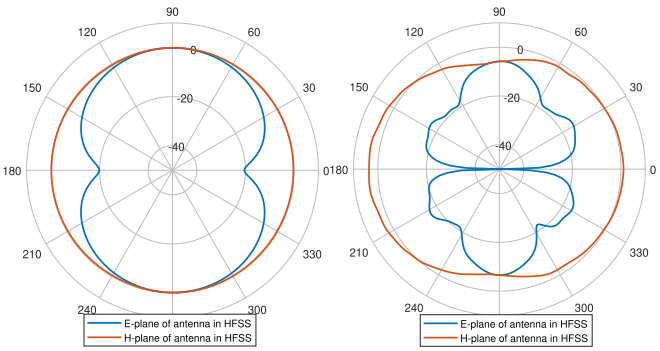

(a) (b)

FIGURE 6. **(a) Simulated E and H plane radiation patterns at 968.8 MHz and (b) 5.5 GHz.**

linear polarization at 5.5 GHz, which proves that the meander and the feed-line of the antenna affect the antenna behavior at the C-V2X bands.

The maximum realized gain of the simulated antenna with the meander at 968.8 MHz is 1.6 dBi and the efficiency 95.4%, as shown in graphs of Fig. 8. At 5.5 GHz the efficiency of the full antenna with the meander is 89.2% and the value of the maximum realized gain is 1 dBi, as indicated in graphs of Fig. 9. At the Figs. 8(a) and 9(a) the realized gain on H-plane is plotted because the Linear Average Gain (LAG) requirements by automotive refer to the gain on H-plane. When the ABS is added below the antenna, the efficiency at 5.9 GHz is 99.7% and the maximum realized gain around 4.2 dBi. After designing the antenna in HFSS, it is fabricated using lithography at Michigan State University. In order to measure the fabricated antenna, an SMA connector is soldered at the pads of the feed-line. The final fabricated antenna with its dimensions is shown in Fig. 1(b) and Table 2.

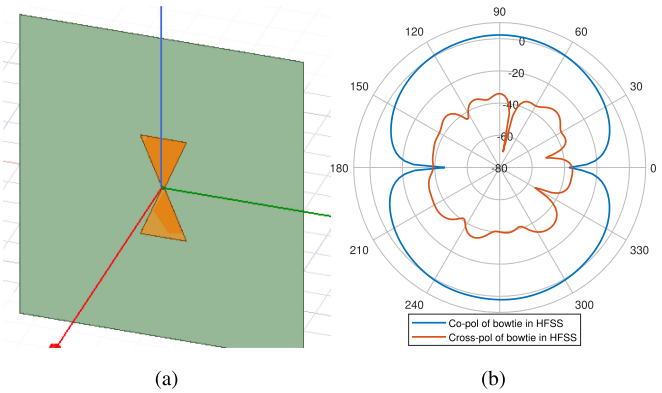

(a) (b)

FIGURE 7. **(a) Bow-tie antenna without the meander line and the slot-line (b) Co and Cross-polarization of the bow-tie on E-plane at 5.5 GHz.**

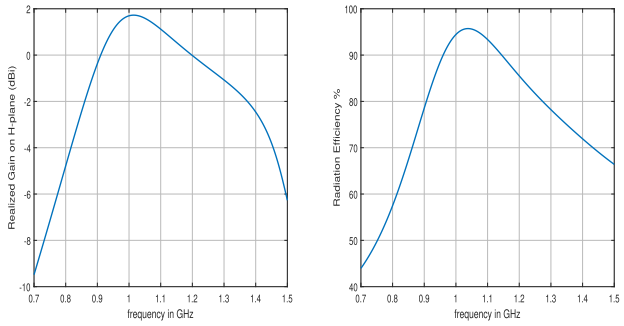

(a) (b)

FIGURE 8. **Graph of the simulated (a) realized gain on H plane and (b) efficiency versus the frequency at cellular bands.**

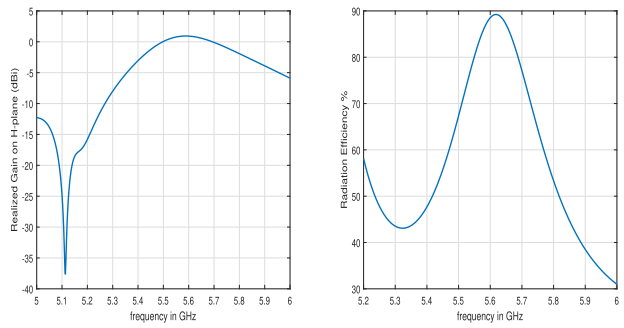

(a) (b)

FIGURE 9. **Graph of the simulated (a) realized gain on H plane and (b) efficiency versus the frequency close to C-V2X bands.**

III. MEASUREMENTS OF ANTENNA

The antenna is measured under four different experimental setups. Initially it is tested in: (a) a SATIMO SG32 near field system at Michigan State University where the far field of the antenna is extracted through the near field spherical measurements and then transferred to Oakland University in order to be measured in their outdoor antenna range facilities as shown in Fig. 10. At Oakland University the antenna is tested; (b) on

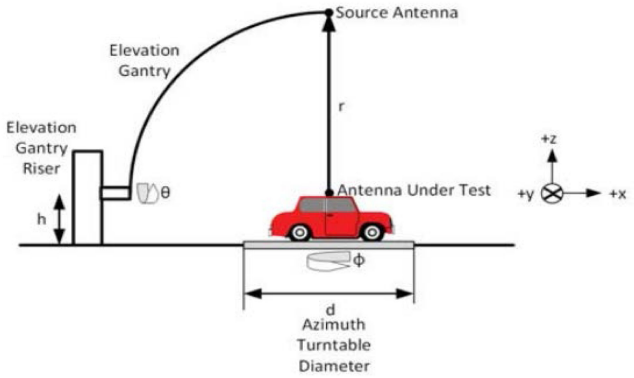

FIGURE 10. Outdoor antenna range measurement facility at Oakland University [16].

FIGURE 11. Antenna placed at the outdoor far field measurement setup of Oakland University without any vehicle.

TABLE 2. Antenna Dimensions in mm

Variable	Dimension (mm)
a	91.5
b	16.5
c	9.5
d	6
e	4
f	10
g	0.5
h	18
j	10

TABLE 3. Comparison of Maximum Co-Polarization Values at the Different Setups and the Values of the Cross-Polarization Where Maximum Co-Polarization Is Achieved

	Cellular		C-V2X	
	Max Co-Pol Value (dBi)	Cross-Pol Value (dBi)	Max Co-Pol Value (dBi)	Cross-Pol Value (dBi)
HFSS	1.6	-22.25	-7.8	-17
SATIMO	1.4	-11.5	-8	-14.2
Oakland No vehicle	1.5	-7.5	4.4	-8.2
Vehicle Mirror	0.8	-2	-0.75	-3.15
Vehicle Trunk	-2.1	-5	0.3	1.04

a stanchion, without the presence of any vehicle; (c) inside the side-mirror cover of a convertible vehicle; and (d) on the trunk lid of the same vehicle. The side mirror as well as the trunk lid are made of ABS material.

The SATIMO SG32 system is covered with absorbers and there are no interventions or barriers to disrupt the antenna's radiation. To measure the antenna at the outdoor facilities without the presence of a vehicle, the antenna is placed on a stanchion on the turntable of Fig. 11. The stanchion is made of non conductive material. Later, a vehicle is added on the turntable of the outdoor antenna range facilities and the antenna is placed inside the side mirror of the co-driver and then on the trunk lid of the vehicle. Measurements for all the mentioned setups are captured and the radiation patterns of the antenna are compared in order to understand how the real environment and the presence of a vehicle affect the antenna characteristics at cellular bands and frequency close to C-V2X band. The maximum values of the co-polarization patterns and the values of the cross-polarization at the same point are indicated in Table 3.

A. ANTENNA MEASUREMENTS IN SATIMO SG32 NEAR FIELD SYSTEM

Before testing the antenna's radiation patterns, the S_{11} of the implemented antenna is measured using the M5227 PNA Network Analyzer by Keysight Technologies. The measurement is shown in Fig. 12. The antenna is placed on a styrofoam inside the Satimo near field system. The measured co-polarization and cross-polarization patterns of the antenna at the cellular (975 MHz) and around the C-V2X frequencies ($5.488\,GHz$), where the antenna resonates, are plotted using Matlab code and are indicated in Fig. 13. These measurements as well as the simulations refer to the realized gain of the antenna. The maximum realized gain of the antenna as measured in SATIMO at 975 MHz is 1.4 dBi and the efficiency is 80%. The LAG of the antenna is 1.13 dBi at 975 MHz. At 5.48 GHz the antenna has a measured efficiency of 70% and a maximum realized gain of 1.2 dBi. At C-V2X frequencies the designed antenna has a LAG of -8 dBi. By introducing an amplifier in

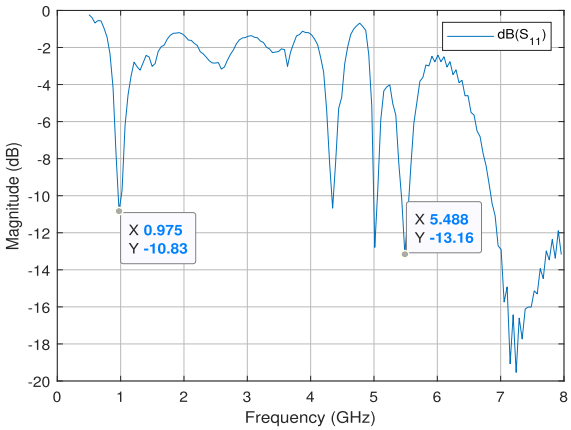

FIGURE 12. PNA measured S_{11}.

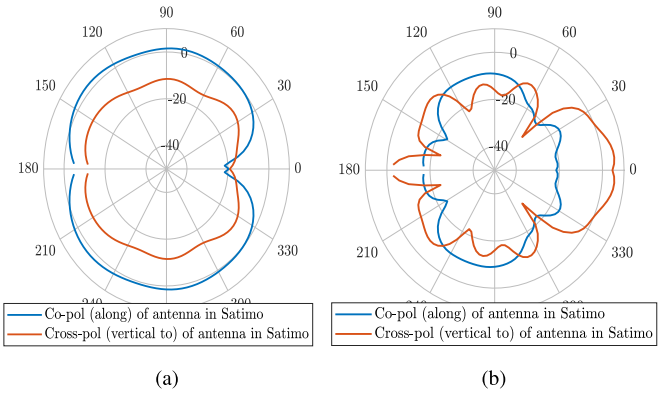

FIGURE 13. Measured co- and cross- polarization gain of implemented antenna (a) at 975 MHz and (b) at 5.5 GHz in Satimo near-field system.

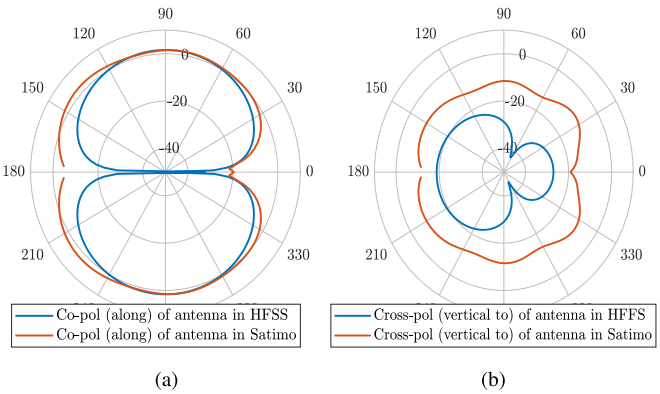

FIGURE 14. Simulated in HFSS and measured in Satimo (a) co- and (b) cross- polarization gain of antenna around 975 MHz.

the structure the transmitted signal at C-V2X frequency can be boosted. The suggested antenna does not have a ground plane and can be mounted on any automotive plastic, which facilitates the use of amplifiers.

When comparing the radiation patterns of the simulated antenna (Fig. 14) to the measurements, there is a reasonable agreement between them. The simulated and measured co-polarization values are almost the same. Namely, in HFSS the highest value of the co-polarization is 1.6 dBi at $\theta = 90^o$ and in Satimo it is measured to be $1.4dBi$ at the same angle at cellular frequencies. However the maximum value of the cross-polarization is higher in the SATIMO measurements (-11.5 dBi) compared to the simulations (-22.25 dBi) around 975 MHz at the same θ. The difference in the averaged cross-polarization values of the simulated and measured antenna is around 7 dBi. At the C-V2X frequencies the measured radiation pattern of the antenna matches the pattern in the simulations and the differences can be explained by the soldering of the SMA connector which cannot be precisely simulated in Ansys EM software, but its size is comparable to the wavelength at 5.5 GHz. In Ansys EM software the soldering was simulated by planar lines, at the edge of the feeding pads connecting the antenna to the SMA connector where in reality the soldering consists of two big bulbs covering the whole area of the feeding pads and extending above the connector. As mentioned in [17] the value of the cross-polarization is affected by the length of the feeding line and the placement of the connector. At 5.5 GHz the simulated co-polarization on E-plane has a maximum value of -7.8 dBi at $\theta = 90^o$ and the cross-polarization on E-plane has a value of -17 dBi at same θ. The maximum value of co-polarization as measured in Satimo anechoic chamber reaches the -8 dBi at same θ value and the cross-polarization is $-14.2-$dBi at the same angle. In order to avoid the radiation pattern deterioration at C-V2X frequency due to the size of the feed-line, an absorbent material can be used to cover the feed-line and eliminate any radiation by it.

B. ANTENNA MEASUREMENTS USING OUTDOOR ANTENNA RANGE FACILITIES OF OAKLAND UNIVERSITY

For the second set of measurements, the antenna is measured at the outdoor range facilities of Oakland University without the presence of a vehicle, as indicated in Fig. 11.

Initially, the antenna is fastened on a stanchion and its co- and cross-polarization radiation patterns on E-plane are measured. The stanchion is placed on a turntable which is conductive, acting as a ground plane. The distance between the antenna and the turntable is 132 cm and the source antenna of Fig. 10 is opposite to the measured antenna, at $\theta = 90^o$. The distance between the antenna and the ground is chosen to be 132 cm because this is equal to the height of the vehicle side mirror from the ground. The co- and cross- polarization of the fabricated antenna are shown in Fig. 16 for the two frequency bands. The antenna patterns are different than what measured in Satimo and simulated in Ansys EM, where there was no ground plane. This is a result of the ground effect. Simulations with the antenna at a distance of 132 cm above an infinite ground plane are performed in HFSS and indicated in Fig. 17. The presence of the ground plane causes an increase in the cross-pol level of the antenna and deteriorates its radiation pattern due to the reflections of the signal on the ground plane. The radiation patterns at the higher frequencies are affected

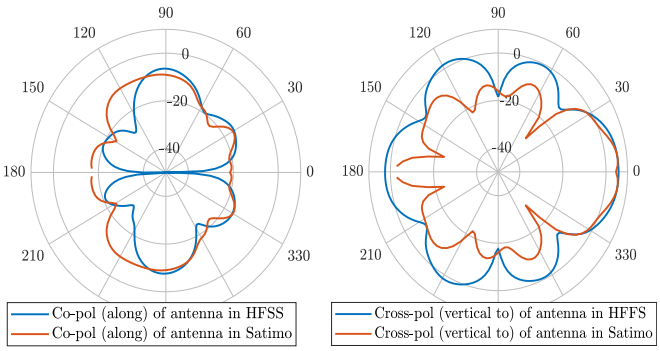

(a) (b)

FIGURE 15. Simulated in HFSS and measured in Satimo (a) co- and (b) cross- polarization gain of antenna around 5.5 GHz.

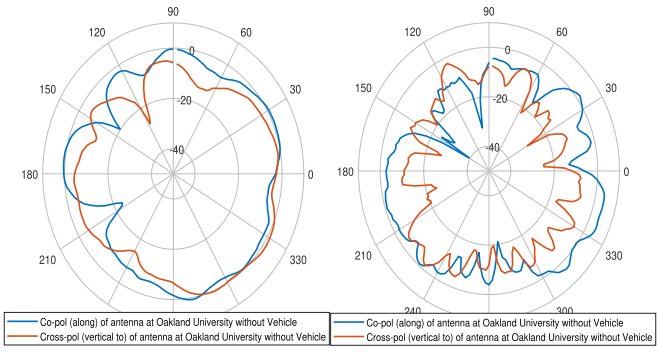

(a) (b)

FIGURE 16. Measured co- and cross- polarization gain patterns of implemented antenna (a) at 960 MHz and (b) at 5.45 GHz at outdoor antenna range facility of Oakland University, without the presence of a vehicle.

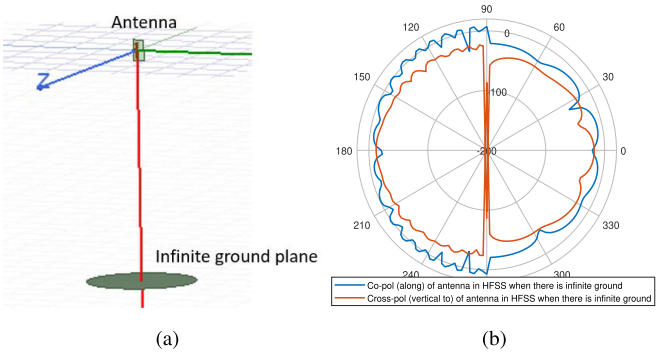

(a) (b)

FIGURE 17. (a) Antenna with infinite ground plane at 132 cm below it in HFSS. (b) Simulated co- and cross- polarization gain patterns of antenna at 984.8 MHz, when there is an infinite ground plane at 132 cm below the antenna.

(a) (b)

FIGURE 18. Antenna placed inside the side-mirror of vehicle.

more than in lower frequencies since, as explained before, the wavelength at higher frequencies is smaller so the effect of the ground and any small obstacles around the antenna becomes more obvious at 5.5 GHz rather than in 960 MHz. For the measurements at cellular frequencies the radiation pattern of the antenna was measured from 800 MHz to 960 MHz with a step of 20 MHz, this is the reason why the measurements at the outdoor facility of Oakland university are plotted at 960 MHz. The co-polarization has a maximum value of 1.5 dBi at $\phi = 10^o$ and the cross-polarization is equal to -7.5 dBi at the same angle at 960 MHz. At 5.5 GHz the co-polarization has a maximum value of 4.4 dBi at $\phi = 334^o$ and the cross-polarization at the same position drops to $-8-$dBi.

At the cellular band, simulations in HFSS with an infinite ground plane below the antenna at a distance of 132 cm are performed. The setup in the HFSS is indicated in Fig. 17(a). The co and cross polarization radiation patterns of the antenna at 984.8 MHz as well as the radiation patterns of the antenna are shown in Fig. 17(b). The simulations are run only for the lower frequency band because the antenna has a linear polarization when there is no ground. The antenna is not linearly polarized at 5.5 GHz even when the ground is missing due to the size of the meander line and of the feed-line. As Fig. 17(b) shows the ground has a significant effect.

C. ANTENNA MEASUREMENTS USING OUTDOOR ANTENNA RANGE FACILITIES OF OAKLAND UNIVERSITY WHEN THE ANTENNA IS PLACED INSIDE THE VEHICLE'S SIDE MIRROR

After measuring the antenna characteristics without a vehicle, a convertible car is added on the turntable and the antenna is positioned inside the side mirror of the passenger, as indicated in Fig. 18. The antenna is placed inside the side mirror cover and the mirror cover is set back on its original position. The mirror cover is made of ABS and is a good candidate to print the antenna on it at a next step. Also by positioning the antenna inside the mirror cover, the antenna radiation can cover the sides and part of the front of the vehicle. The co- and cross-polarization patterns of the antenna for the different frequency bands can be found in Fig. 19. The co- and cross-polarization of the antenna are plotted for $\theta = 90^o$ which means that the transmitter/source antenna of Fig. 10 is at the same level with the car. During our experiments, in contrast to Fig. 10, the Antenna Under Test (AUT) is not placed on the rooftop of the car but inside the side-mirror cover and then on

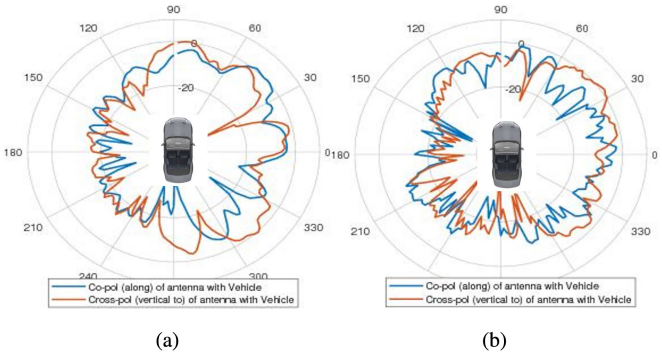

FIGURE 19. Measured co- and cross- polarization of implemented antenna (a) at 960 MHz and (b) at 5.9 GHz at the outdoor antenna range facility of Oakland University, when the antenna is inside the side-mirror cover of a vehicle.

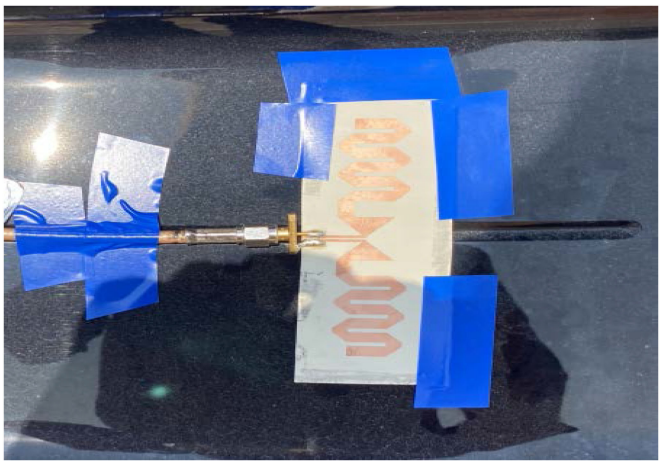

FIGURE 20. Antenna placed on the trunk lid of the vehicle.

the trunk lid of the vehicle. At cellular frequencies, when the antenna is placed inside the side mirror, the maximum value of co-polarization is 0.8−dBi at $\phi = 48^o$. The cross-polarization at same position is measured around −2 dBi at 960 MHz. At 5.9 GHz the max value of the co-polarization is −0.75 dBi at $\phi = 350^o$ and the cross-polarization at the same angle is −3.15 dBi.

D. ANTENNA MEASUREMENTS USING OUTDOOR ANTENNA RANGE FACILITIES OF OAKLAND UNIVERSITY WHEN THE ANTENNA IS PLACED ON THE VEHICLE'S TRUNK LID

For the last set of experiments the antenna is taped on the trunk lid of the vehicle as shown in Fig. 20. The cross- and co-polarization of the AUT for $\theta = 90^o$ of the source antenna, at 960 MHz and 5.9 GHz is plotted and shown in Fig. 21. As indicated, at 960 MHz the maximum co-polarization value is −2 dBi at $\phi = 90^o$ and the cross-polarization at same angle is −5 dBi. At 5.9 GHz the co-polarization has a maximum value of 0.3 dBi at $\phi = 124^o$ where the cross-polarization is 1.04 dBi.

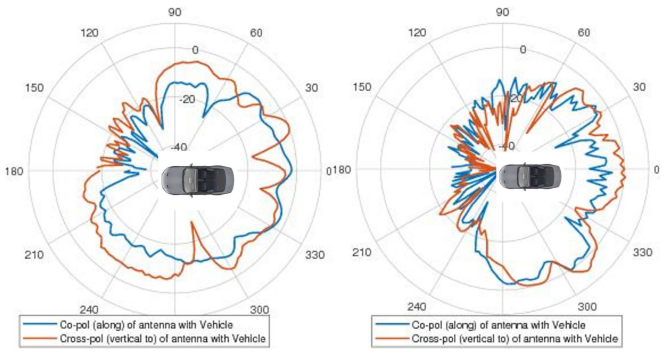

FIGURE 21. Measured co- and cross- polarization of implemented antenna (a) at 960 MHz and (b) at 5.9 GHz at outdoor antenna range facility of Oakland University, when the antenna is placed on the trunk lid of the vehicle.

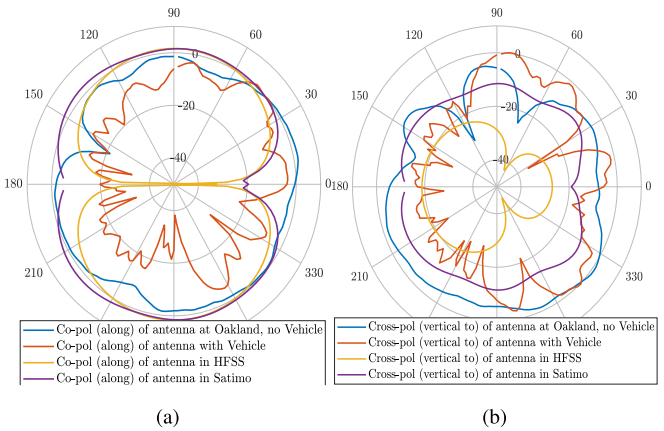

FIGURE 22. Comparison of antenna (a) co- and (b) cross- polarization as simulated in HFSS, as measured in Satimo system and as at the outdoor facility without and with a vehicle, when antenna is placed inside the mirror cover, at cellular band.

IV. COMPARISON OF RESULTS AND CONCLUSION

A. COMPARISON OF ANTENNA CO- AND CROSS-POLARIZATION AT THE FOUR DIFFERENT EXPERIMENTAL SETUPS

To compare the co- and cross-polarization values at the different experimental setups the data indicated in Figs. 3, 13, 16, 19 and 21 are gathered, separated to co-polarization and cross-polarization radiation patterns and are presented in Figs. 22, 23, 24 and 25.

When comparing the co- and cross-polarization gain patterns of the antenna at the different experimental setups in cellular frequency bands, it is obvious that although the antenna has a linear polarization when simulated and measured in the Satimo system, without a ground plane, the cross-polarization level increases when exposed to open space, with or without a vehicle due to the ground effect. As a result the direction of polarization has been shifted.

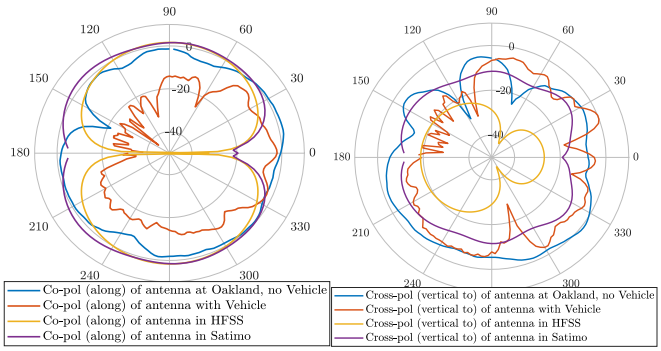

FIGURE 23. Comparison of antenna (a) co- and (b) cross- polarization patterns as simulated in Ansys HFSS, as measured in Satimo system and at the outdoor facility without and with a vehicle, when antenna is placed on the trunk lid at cellular bands.

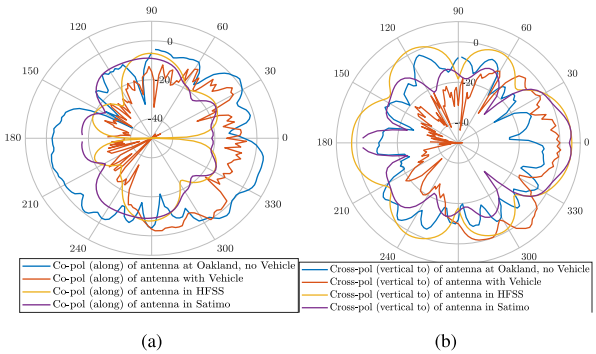

FIGURE 25. Comparison of antenna (a) co- and (b) cross- polarization patterns as simulated in HFSS, as measured in Satimo system and at the outdoor facility without and with a vehicle, when antenna is placed on its trunk lid at C-V2X band.

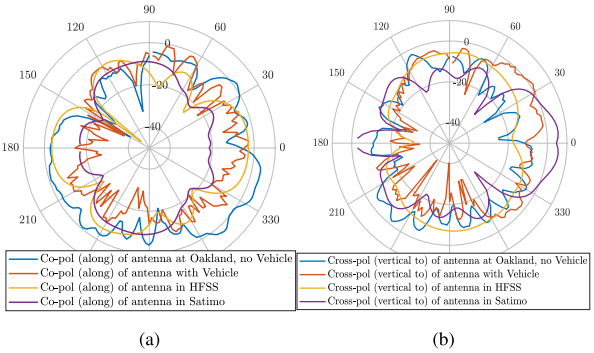

FIGURE 24. Comparison of antenna (a) co- and (b) cross- polarization patterns as simulated in HFSS, as measured in Satimo system and at the outdoor facility without and with a vehicle, when antenna is placed inside the side-mirror cover, at C-V2X band.

Figs. 2 and 12 show the resonance frequencies of the simulated and the implemented antennas as measured in the lab using the M5227 PNA Network Analyzer of Keysight Technologies. The simulated and the implemented antennas resonate at 984.8 MHZ and 975 MHz respectively for the cellular bands. Also, both of them have $S_{11} < -10\,dB$ at 5.5 GHz. The resonance frequencies of the simulated and the implemented antennas are the same.

In Figs. 14 and 15 the co and cross- polarization radiation patterns of the simulated antenna and the implemented one as measured in Satimo system are gathered in the same plot. In these figures it is obvious that the radiation patterns of the simulated and measured antennas show reasonable agreement. The average cross-polarization of the implemented antenna at the cellular bands is 7 dB higher than the simulated. At 5.5 GHz the cross-polarization is high because the size of the meander and the feeding line are not negligible when compared to the wavelength. Each automotive company has set its own standards on the required antenna gain. To improve the deterioration of the antenna radiation pattern at C-V2X frequency, an absorbing material can be used to cover the feed-line. Moreover, further investigation can be performed in identifying a suitable feed method for this antenna that will not interfere with its performance at the higher frequency band.

At cellular frequencies the maximum co-polarization values when the antenna is measured in the Satimo system and at the Oakland outdoor range facility, presented in Fig. 16, are close to the simulated value of 1.6 dBi with a deviation less than 0.2 dBi, as indicated in Table 3. The radiation patterns of the antenna when measured alone at the outdoor measurement setup of Oakland are different compared to the radiation patterns of the antenna when measured in Satimo near field system. The difference in the patterns is caused by the metallic turntable on which the antenna is placed and acts as a ground plane. Simulations with the antenna 132 cm above a round ground plane are indicating that the patterns of the antenna are affected when there is ground below it, as shown in Fig. 17. As stated in [18] the diffracted fields of the ground affect the pattern and the values of the cross-polarization. The simulated maximum value of the co-polarization at 984.8 MHz when there is ground below it, is 7 dBi but it has many lobes due to reflections. The antenna loses its linearity and the cross-polarization increases to -13 dBi at 180^o, close to the co-polarization values.

When the antenna is mounted on the trunk lid of the vehicle, we get the minimum value of the co-polarization radiation pattern on E-plane at cellular frequencies. The closest the antenna is on the ground, the least is the value of the realized gain and the higher the value of the cross-polarization because as stated in [19] and [18] the surface waves propagating along the ground affect the level of cross polarization. The difference between the co-polarization and cross-polarization values decreases when the vehicle is added in the experimental setup. When the antenna is measured on the car, there are huge metal surfaces around it because of the vehicle's body which creates many reflections and deformities to the antenna radiation pattern as indicated in Figs. 19 and 21.

When comparing the antenna radiation pattern of the four measurement setups, it is obvious that the reflections due to the outdoor space, presence of ground plane and vehicle body disturb the antenna polarization resulting in loss of antenna linearity, at cellular frequencies as indicated in Fig. 22.

When placing the antenna on the vehicle's trunk lid, we get similar results as indicated in Figs. 21, 23 and 25. The difference between placing the antenna on the trunk lid and placing it inside the side-mirror cover is that the trunk lid is closer to the turn-table and ground. As a result there are reflections affecting the antenna's radiation pattern and the values of the co- and cross- polarization patterns are deviating more from the simulated values when compared with the other experimental setups. At 5.9 GHz the maximum value of the cross-polarization of the antenna exceeds the maximum value of the co-polarization.

The antenna's radiation pattern is distorted at the higher frequency bands. The antenna at 5.9 GHz is not designed to be linearly polarized due to the SMA connector, the size of the feedline and the meander lines, which are comparable to the wavelength since the cross-polarization is created due to the transverse currents of the higher order modes. In Figs. 24 and 25 the co- and cross-polarization of the antenna as simulated in Ansys EM (HFSS) and measured during the various experimental setups is indicated. The measured maximum values of the co-polarization are higher than the simulated. The reflections created by the obstacles in the real environment, the ground and the vehicle's body modify the antenna's radiation patterns and add more to its maximum radiation pattern values. The smallest value of the cross-polarization at the angle where we have the maximum co-polarization value at 5.9 GHz, when the vehicle is present, is measured to be −3.15 dBi when the antenna is placed inside the mirror's cover. At that placement the antenna is higher from the ground, compared to the trunk lid position, but the conductive body of the vehicle is closer to the antenna. As stated in [19] and [18] the presence of ground causes the generation of higher level cross-polarization due to surface waves propagating along the ground. For this reason, the values of the cross-polarization increase when the vehicle is added, compared to the measurements on the stanchion and in the Satimo system.

B. CONCLUSIONS

The antenna presented in this paper was mounted inside a mirror cover and on the trunk lid of a convertible car to measure the effect of the ground and the vehicle body on the transmission and reception of microwave signals. The results of the experiments at the outdoor antenna range facility showed that this flexible, dual-band antenna can be mounted on any automotive plastic part and does not require a shark fin or a ground plane. The radiation performance of the antenna was measured. The Linear Average Realized Gain (LAG) of the antenna is 1 dBi at 975 MHz and −8 dBi around 5.5 GHz as measured in Satimo system. By the use of a suitable amplifier the power of the antenna's signal at C-V2X can be boosted and compensate for the low gain. Through the Friis transmission formula the required amount of signal can reach the receiver at C-V2X, even though the antenna gain is low.

From the experiments performed it is proved that at lower cellular frequencies the cross-polarization of the designed antenna is mostly affected by the ground plane since the presence of the ground increases the cross-polarization values. Moreover, the vehicle's body affects the radiation patterns of the antenna by creating more nulls due to the escalated number of reflections. At higher frequency bands, close to C-V2X, the antenna radiation pattern is affected more compared to the lower frequencies because of the smaller wavelength. So the car's body and ground perturb the antenna radiation substantially. When comparing the two candidate positions for antenna placement (side mirror cover and trunk lid), the mirror cover is preferable. This placement is higher than the trunk lid, which means it is further from the ground. To minimize signal degradation due to the body of the vehicle, another similar antenna can be placed inside the driver's mirror cover, thus, improving the overall area coverage.

The antenna suggested in this paper is a lightweight antenna, with no ground. It can be placed at any automotive plastic part and it does not restrict its use inside the shark fin on the rooftop of a vehicle. The microwave signal transmission and reception of this antenna is perturbed by the presence of the ground and the vehicle's body but using an amplifier and a second antenna on the other side mirror the signal disruption can be minimized.

ACKNOWLEDGMENT

The authors would like to thank Dr. Daniel Aloi and Ahmed Harb for the measurements in the outdoor range facility of Oakland University. The authors also like to acknowledge the support of Ford Motor Company for this project.

REFERENCES

[1] Z. Huang, Y. Li, R. Chen, and M. Yang, "Clustering analysis of multipath components in urban road scenario for C-V2X propagation channels," in *Proc. IEEE 12th Int. Symp. Antennas, Propag. EM Theory*, 2018, pp. 1–3.

[2] T. Izydorczyk, F. M. L. Tavares, G. Berardinelli, M. Bucur, and P. Mogensen, "Performance evaluation of multi-antenna receivers for vehicular communications in live LTE networks," in *Proc. IEEE 89th Veh. Technol. Conf.*, 2019, pp. 1–6.

[3] F A. Saccardi *et al.*, "Virtual drive testing based on automotive antenna measurements for evaluation of vehicle-to-X communication performances," in *Proc. IEEE Int. Symp. Antennas Propag. USNC-URSI Radio Sci. Meeting*, 2019, pp. 927–928.

[4] S. Senega, J. Kammerer, and S. Lindenmeier, "Scan-phase antenna diversity for digital satellite radio (SDARS) in a single automotive side mirror," in *Proc. 8th Eur. Conf. Antennas Propag.*, 2014, pp. 3255–3259.

[5] T. Abbas, J. Karedal, and F. Tufvesson, "Measurement-based analysis: The effect of complementary antennas and diversity on vehicle-to-vehicle communication," *IEEE Antennas Wireless Propag. Lett.*, vol. 12, pp. 309–312, 2013.

[6] S. Imai, K. Taguchi, T. Kashiwa, and T. Kawamura, "Effects of car body on radiation pattern of car antenna mounted on side mirror for inter-vehicle communications," in *Proc. IEEE Antennas Propag. Soc. Int. Symp.*, 2014, pp. 601–602.

[7] L. Marantis, A. Paraskevopoulos, D. Rongas, A. Kanatas, C. Oikonomopoulos-Zachos, and S. Voell, "A printed monopole espar antenna for truck-to-truck communications," in *Proc. Int. Workshop Antenna Technol., Small Antennas, Innov. Struct., Appl.*, 2017, pp. 239–242.

[8] S. N. Hasnain, R. Stephan, M. Brachvogely, M. Meureryz, and M. A. Hein, "Interference mitigation for robust automotive satellite navigation achieved with compact distributed antenna sub-arrays," in *Proc. IEEE 14th Eur. Conf. Antennas Propag.*, 2020, pp. 1–5.

[9] D. Pototzki and A. Griesche, "Exploring radiating and scattering sources of part of vehicles by means of hemi-spherical-near-field antenna measurements," in *Proc. 6th Eur. Conf. Antennas Propag.*, 2012, pp. 2249–2251.

[10] M. B. Diez, W. Pascher, and S. Lindenmeier, "Electromagnetic characterization of automotive sunroofs for car-to-X applications," in *Proc. 46th Eur. Microw. Conf.*, 2016, pp. 1323–1326.

[11] S. Hastürkoğlu, M. Almarashli, and S. Lindenmeier, "A compact wideband terrestial MIMO-antenna set for 4G, 5G, WLAN and V2X and evaluation of its LTE-performance in an urban region," in *Proc. 13th Eur. Conf. Antennas Propag.*, 2019, pp. 1–5.

[12] H. Tazi, C. Ullrich, and T. F. Eibert, "Virtual development of automotive antennas printed on glass using a hybrid of method of moments and method of auxiliary sources," in *Proc. Asia-Pacific Microw. Conf.*, 2011, pp. 614–617.

[13] M. Almarashli and S. Lindenmeier, "A new method for evaluation of LTE MIMO antennas in automotive application," in *Proc. 11th Eur. Conf. Antennas Propag.*, 2017, pp. 2450–2453.

[14] A. Chletsou, Y. He, J. F. Locke, and J. Papapolymerou, "Multi-band, flexible, lightweight antenna on LCP for automotive applications," in *Proc. IEEE Int. Symp. Antennas Propag. North Amer. Radio Sci. Meeting*, 2020, pp. 1507–1508.

[15] Rogers Corporation. Datasheet of Rogers 3850 Dielectric, [Online]. Available: https://www.midwestpcb.com/data sheets/Rogers ULTRALAM.pdf

[16] N. D. Aloi and E. Abdul-Rahman, "Modeling of a far-field automotive antenna range using computational electromagnetic tools," in *Proc. 14th Eur. Conf. Antennas Propag.*, 2020, pp. 1–5.

[17] H. Jingjian, Z. Xiaofa, X. Shaoyi, W. Weiwei, and Y. Naichang, "Suppression of cross-polarization of the microstrip integrated balun-fed printed dipole antenna," *Int. J. Antennas Propag.*, vol. 2014, pp. 1–8, 2014.

[18] J. L. Salazar, N. Aboserwal, J. D. Díaz, J. A. Ortiz, and C. Fulton, "Edge diffractions impact on the cross polarization performance of active phased array antennas," in *Proc. IEEE Int. Symp. Phased Array Syst. Technol.*, 2016, pp. 1–5.

[19] A. B. Smolders, R. M. C. Mestrom, A. C. F. Reniers, and A. Zamanifekri, "Effect of a finite ground plane on the axial ratio of circularly-polarized microstrip arrays," in *Proc. Eur. Microw. Conf.*, 2013, pp. 203–206.